A Novel Bidirectional Output Oscillating-Amplifying Integrated Fiber Laser With 2 Ports × 2 kW Level Near-Single-Mode Output

Jiaqi Liu, Lingfa Zeng, Peng Wang, Baolai Yang, Xiaoming Xi, Chen Shi, Hanwei Zhang, Xiaolin Wang, and Fengjie Xi

***Abstract*—A novel bidirectional output oscillating-amplifying integrated fiber laser which combines the advantages of the bidirectional output fiber laser oscillator and the oscillating-amplifying integrated fiber laser is proposed and demonstrated experimentally. The influences of the reflectivities and center wavelengths of FBGs on the laser output power and efficiency were studied theoretically. The characteristics of the output laser were studied in detail in experiment. Based on this structure, we finally demonstrated a bidirectional laser output of 2 × 2-kW level with an active fiber length of 6 m for the oscillating section and 7 m for the amplifying section at both ends. The optical-to-optical conversion efficiency is 80.4%. The beam qualities of both ends are $M_A^2 \sim 1.3$ and $M_B^2 \sim 1.4$, which indicates a near-single-mode output. To the best of our knowledge, it was the first time that this structure has been proposed, and its feasibility was demonstrated experimentally.**

***Index Terms*—Fiber laser, high power laser, bidirectional oscillating-amplifying integrated structure, ytterbium-doped fiber.**

I. Introduction

FIBER lasers have the advantages of high conversion efficiency, good beam quality, compact structure, and convenient thermal management [1], [2]. In the past decades, benefited from the development of high-brightness, high-power pumping technology and advanced manufacturing technology of double-clad Ytterbium-doped fiber (DCYDF) with large mode area (LMA), the output power of fiber lasers has been rapidly increased which has promoted the fast-rising development of high-power fiber lasers [3], [4]. Nowadays, high-power fiber lasers have become one of the preferred light sources for many laser systems, and have been widely used in industrial processing, medical, scientific research, and many other fields [4]. The traditional structure of the fiber laser oscillator is composed of a high-reflectivity fiber Bragg grating (HR-FBG), an output coupler fiber Bragg grating (OC-FBG), and an active fiber. Since the HR-FBG cannot reach a reflectivity of 100%, there will be a small part of laser transmitted through the HR-FBG, which can hardly be used. In applications where the power requirement is not high, multichannel laser can be obtained through the devices such as combiners and couplers [5]. However, these methods will result in an increase of the volume of the system with the number of fiber lasers as well as being limited by the power capability of the coupling devices. Considering the factors of cost, efficiency, structural volume and weight, the researchers modified the structure of traditional unidirectional output fiber laser oscillator and proposed a fiber laser with bidirectional output. According to published reports, except for using space lens to reflect and couple the laser output at different angles in the early years [6], [7], [8], there are three ways to achieve bidirectional laser output. The first method is to separate the laser into clockwise and counterclockwise transmission and then output in a ring laser [9], [10], [11]. It's currently the most prevalent method to achieve bidirectional output of fiber lasers. The second method uses a dual-core fiber to achieve the non-coaxial parallel transmission of pumping light and signal light in the core of active fiber and power-transmitting fiber, respectively [12]. Setting the reflectivity and bandwidth of the fiber Bragg gratings (FBG) uniformly, bidirectional symmetrical power output can be obtained. The third method achieves bidirectional output in an all-fiber linear cavity composed of a double-clad monolithic Ytterbium-doped fiber [13], [14]. Fig. 1 shows a schematic diagram of the bidirectional all-fiber linear cavity fiber laser structure. The resonant cavity is composed of two FBGs and a section of active fiber. Laser transmits back and forth in the resonant cavity, being reflected and coupled by FBGs, finally output from quartz block head (QBH) of each end. In 2022, Zhong et al. achieve a 2 × 2kW near-single-mode bidirectional output on this structure [14]. However, both OC-FBGs structure in the bidirectional fiber laser resonator led to less round-trips times of laser in the cavity, finally resulting in low utilization of pumping. In order to increase the transverse mode instability (TMI) threshold and pumping utilization of fiber laser oscillators, Hejaz et al. proposed the oscillating–amplifying integrated fiber laser

Manuscript received 21 September 2022; revised 3 November 2022; accepted 14 December 2022. Date of publication 19 December 2022; date of current version 9 January 2023. This work was supported by the Training Program for Excellent Young Innovations of Changsha under Grant kq2106008. *(Jiaqi Liu and Lingfa Zeng are co-first authors.) (Corresponding authors: Xiaolin Wang; Fengjie Xi.)*

The authors are with the College of Advanced Interdisciplinary Studies, National University of Defense Technology, Changsha 410073, China, also with the Nan Hu Laser Laboratory, Changsha 410073, China, and also with the Hunan Provincial Key Laboratory of High Energy Laser Technology, Changsha 410073, China (e-mail: 942834358@qq.com; zenglingfa14@nudt.edu.cn; 1169723259@qq.com; yangbaolai1989@163.com; exixiaoming@163.com; bigbryant@nudt.edu.cn; zhanghanwei100@163.com; chinawxllin@163.com; xifengjie@163.com).

Digital Object Identifier 10.1109/JPHOT.2022.3230376

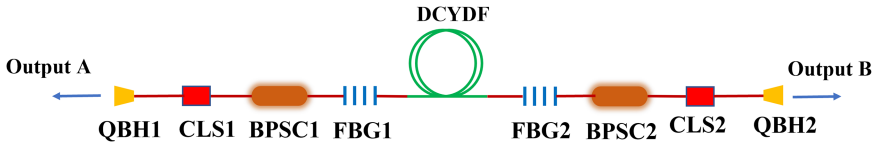

Fig. 1. Schematic diagram of the bidirectional all-fiber linear cavity fiber laser structure.

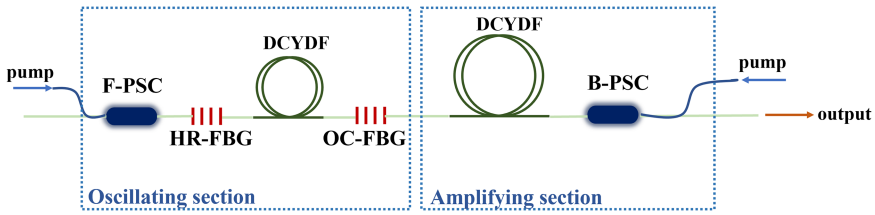

Fig. 2. Structure of oscillating–amplifying integrated fiber laser.

TABLE I
THE MAIN PARAMETERS OF THE SIMULATION

Name	Number	Unit
Pump wavelength	976	nm
Pump power of end A	2400	W
Pump power of end B	2400	W
Core/cladding diameters	22/400	μm
Overlap factor of pump	0.0025	
Overlap factor of signal	1	
Length of DCYDF	6	m
Length of DCYDF-A	7	m
Length of DCYDF-B	7	m
Fiber absorption	1.62	dB/m
Radiative lifetime	8×10^{-4}	s
Central output wavelength	1080	nm

(OAIFL), which increased the TMI threshold by about 26% [15]. Fig. 2 shows the structure of oscillating-amplifying integrated fiber laser. This new structure consists of an oscillating section and an amplifying section. It conspicuously removes the isolator or cladding light stripper (CLS) between the oscillating section and the amplifying section of the traditional fiber laser amplifier based on master oscillation power amplification (MOPA) which allows the pumping light of forward and backward to obtain a higher utilization, thereby this new structure laser has a higher efficiency [16]. At the same time, the backward light can be reflected by HR-FBG and further amplified in the amplifying section, finally output as target laser, which ensures the good anti-back-reflected light ability of the traditional oscillator [17].

In this paper, on the basis of bidirectional output fiber laser oscillator, considering the advantages of the oscillating-amplifying integrated fiber laser, we propose a new structure and name it as bidirectional output oscillating-amplifying integrated fiber laser(B-OAIFL). This new structure can theoretically combine the advantages of bidirectional output fiber laser and oscillating-amplifying integrated fiber laser, which includes high efficiency, high stability, good anti-backreflection and control logic simplicity, etc. We first study theoretically the effect of the reflectivity and center wavelengths of the FBG on the output power and efficiency. At the same time, we focus on factors such as the stability threshold and TMI threshold of the laser to optimize the parameters of the resonant cavity. By optimizing the relevant parameters, the feasibility of the B-OAIFL structure is verified experimentally for the first time, a bidirectional 2-kW-level near-single-mode ($M_A^2 \sim 1.3$, $M_B^2 \sim 1.44$) output is realized with an O-O efficiency of 80.4%.

II. CONFIGURATION AND SIMULATION OF THE B-OAIFL

Fig. 3 shows the model of the B-OAIFL in the fiber laser simulation software SeeFiberLaser. This novel structure is mainly divided into an oscillating section and two amplifying sections at both ends, its structure diagram is shown in the figure. A piece of DCYDF and a pair of FBGs form the oscillating section. Both ends of DCYDF are fusion spliced to FBG, respectively. The other ends of the two FBGs are fusion spliced with a piece of DCYDF to compose the amplifying section, the laser output from the oscillating section will be further amplified in this section. The other ends of DCYDF of the amplifying section are fusion spliced to the backward pump/signal combiner (BPSC), all the LDs are combined through the BPSC and injected into the laser as the pump source. The laser passes through a piece of passive fiber with the CLS, outputs from the QBH, and then enters the measuring system. According to theoretical analysis, there are plenty of potential advantages in this novel structure. Compared with the unidirectional OAIFL, there is an increase in the number of output end, a bidirectional laser output with high power can be achieved by performing a laser, which promotes the

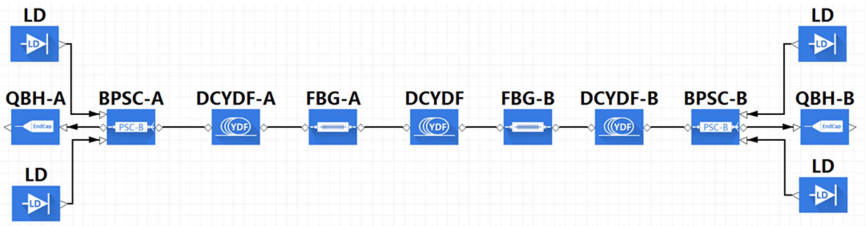

Fig. 3. Configuration and model in SeeFiberLaser.

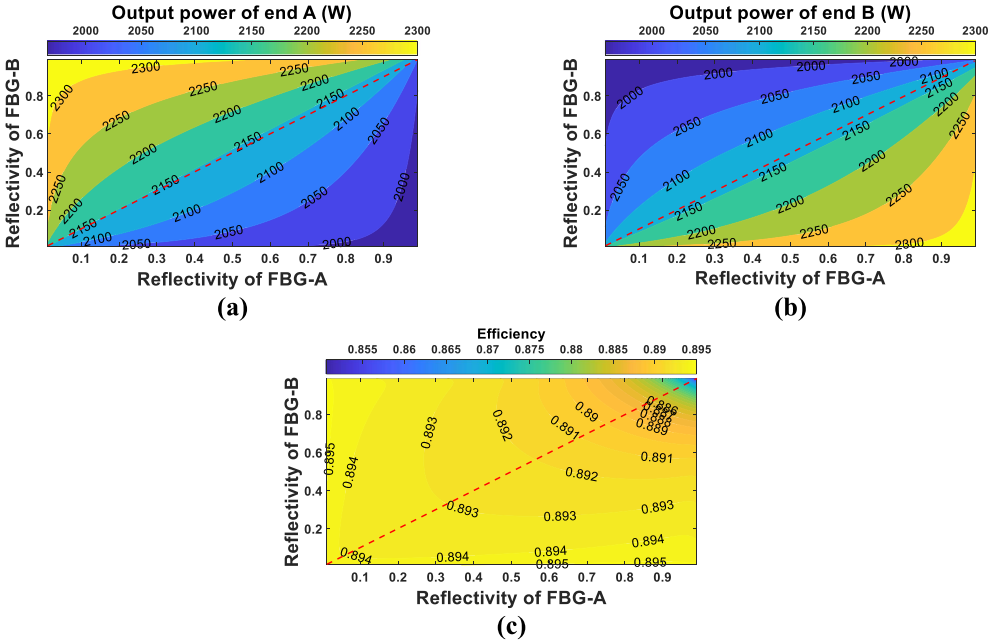

Fig. 4. The simulation results of output power and efficiency as a function of FBGs. (a) The output power of end A varies with the reflectivity of FBGs. (b) The output power of end B varies with the reflectivity of FBGs. (c) The O-O efficiency varies with the reflectivity of FBGs.

reduction of the cost and the volume simplification of the system. Compared with the bidirectional linear-cavity laser oscillator, the highlight spot of the B-OAIFL is its higher efficiency lead by the higher utilization of pump light. Due to the existence of the amplifying section at both ends, the pump light is further utilized, and the laser output from the oscillator is fully amplified, so that makes it theoretically realize the promotion of the efficiency, and achieve a higher output power at the same pump level. Benefiting from the guaranteed amplification of the amplifying section, the length of active fiber in the oscillating section can be as short as possible under the consideration of the ASE suppression and the stability, and the pump light will be fully absorbed when it passes through the amplifying section. All these characteristics lead a lower power of the cavity, which contributes to the reduction of the requirement of the FBGs. Besides, according to the analysis of the structure, due to the sufficient absorption of the amplifying section, the pump light of one end shows little effect on the other end, based on it, the B-OAIFL can allow a more flexible arrangement of pump energy to realize a simple adjustment of bidirectional output power.

The influence of the reflectivity of FBGs on output power and efficiency of the B-OAIFL is studied in the fiber laser simulation software named SeeFiberLaser. In theory, the power of each LD is 1200 W with a center wavelength of 976 nm. The transmission efficiency of BPSC1 and BPSC2 for signal light is 100%, and as well as for the pump light. The center wavelengths of FBG-A and FBG-B are 1080 nm with reflectivities which can be adjusted in the range of 1% to 99%. The main parameters of the simulation are shown in Table I.

Varies the reflectivity of both FBG-A and FBG-B in the range of 1% to 99%, the output power and the O-O efficiency are studied. Fig. 4 shows the variations of output power and O-O efficiency vary with the reflectivity of FBGs in the form of contour maps. As we can see from the Fig. 4(a), (b), fixing the reflectivity of FBG at one end, the output power of this end shows a positive correlation with the reflectivity of FBG of the other end, however, the output power of the other end is opposite. Besides, fixing the reflectivity of FBG-A and FBG-B at an equal value which is shown by the red dot line in Fig. 4, a bidirectional output with almost equal power can

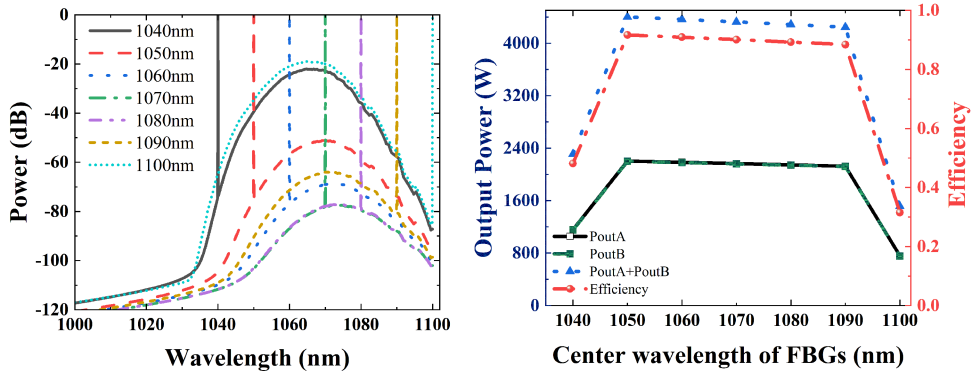

Fig. 5. The simulation results of the effect of the center wavelength of the FBGs on ASE suppression: (a) The intensity of the ASE at several center wavelength of FBGs; (b) The variation of output power and efficiency with the center wavelength of FBGs.

TABLE II
SIMULATION OUTPUT PARAMETERS OF B-OAIFL AT DIFFERENT CENTER WAVELENGTH ON FBGS

Center wavelength/nm	Relative intensity of ASE/dB	Optical-to-optical efficiency	Output power of signal light/W
1040	-22.12	0.4814	2310.72
1050	-51.14	0.9165	4399.59
1060	-68.6	0.9093	4364.44
1070	-77.5	0.9009	4324.50
1080	-77.16	0.8926	4284.41
1090	-63.82	0.8841	4243.79
1100	-19.07	0.3153	1513.50

be achieved, and it negatively related to the reflectivity of the FBGs. Similarly, the O-O efficiency shows a few drops as the reflectivity of FBG increases, as is shown in Fig. 4(c).

Furthermore, the influence of the center wavelengths of FBGs on the suppression of amplified spontaneous emission (ASE), output power and efficiency are theoretically studied. The reflectivity of FBGs is fixed at 10%, and the remaining parameters are consistent with the above, Fig. 5 shows the theoretical results when changing the center wavelength of FBGs from 1040 nm to 1100 nm. The results in Fig. 5(a) indicates a negative correlation of the intensity of ASE with the center wavelength of FBGs in the range from 1040 nm to 1070 nm. We can see that a strong ASE occurs at the wavelength of 1040 nm, as the wavelength increases, it gradually weakens, and almost disappears in the wavelength range of 1070 nm-1080 nm. When the central wavelength exceeds 1090 nm, the obvious ASE reappears and increases rapidly when the central wavelength increases to 1100 nm. Considering that the ASE is unnecessary and needs to be suppressed in practice, we exclude the proportion of it when calculating the output power and O-O efficiency in simulation. We calculate the power in the range of 0.5 nm on each side of the center wavelength of output laser, regard it as the signal light power, and calculate the corresponding O-O efficiency, the results are depicted in Fig. 5(b), which shows the output power of signal light and its corresponding O-O efficiency as a function of the center wavelength of FBGs, it is worth noting that there is a strong ASE at the center wavelength of 1040 nm with a suppression ratio of 22.12 dB and a power proportion of 47.43%, which results in a relatively low efficiency about 48.14%. As the center wavelength of FBGs increases, due to the reduced proportion of ASE of the output laser, there is a great improvement in efficiency, which achieves 91.65% at 1050 nm. In the wavelength range of 1050 nm to 1090 nm, the output power and efficiency decrease slightly with the increase of wavelength, but remain at a stable level. However, both output power of the signal and the O-O efficiency show a significant drop in the wavelength range of 1090 nm to 1100 nm which is believed to be caused by the same reason as at 1040 nm. Simulation results of B-OAIFL at different center wavelengths of FBGs are summarily shown in Table II. According to the analysis of the simulation results, a conclusion can be drawn: in order to achieve as high as possible bidirectional output power, the FBGs with the center wavelength in the range from

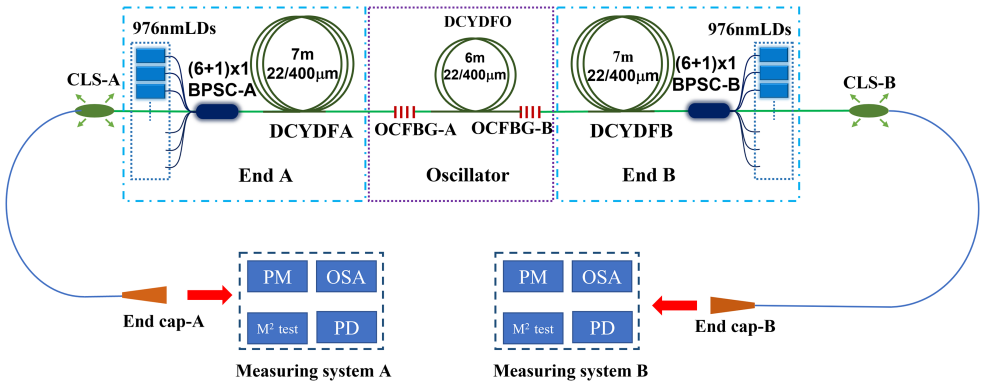

Fig. 6. Experimental structure of B-OAIFL.

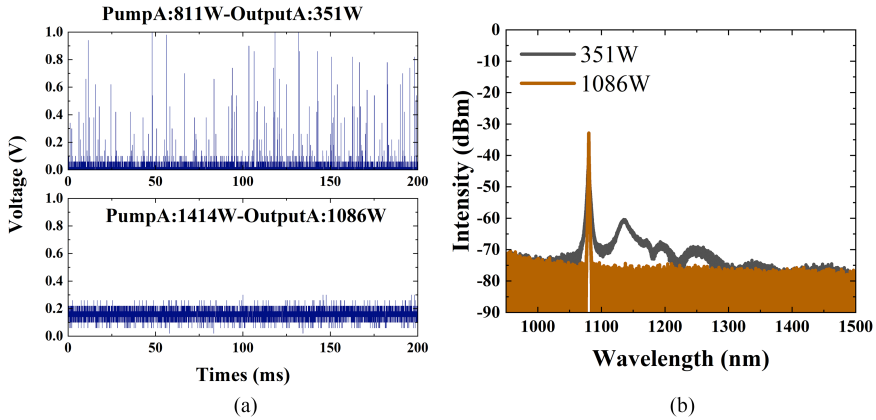

Fig. 7. Experimental results before and after the stabilization of B-OAIFL: (a) Characteristics of the time-domain; (b) Characteristics of the output spectrum.

1070 nm to 1080 nm should be adopted, and the reflectivity of FBG should be as low as possible under the condition of no ASE.

III. Experimental Setup

The experimental structure of B-OAIFL is shown in Fig. 6. This laser consists of three sections: oscillating section and two amplifying sections which are named end A and end B, respectively. The active fiber of this structure is a DCYDF with a core/inner-cladding diameters of 22/400 μm and a normal cladding absorption coefficient of 1.62 dB/m@976 nm. The oscillating section is composed of a 6 m-long DCYDF and a pair of 22/400 μm OC-FBGs. The center wavelength of OCFBG-A is 1079.86 nm with a reflectivity of 9.7% and a 3 dB bandwidth of 1 nm. The center wavelength of OCFBG-B is 1079.94 nm with a reflectivity of 8.5% and a 3 dB bandwidth of 1.1 nm. All these three devices make up the oscillating section of the laser. The amplifying section at both ends of oscillating section are composed of a 7 m-long DCYDF (DCYDFA, DCYDFB), a (6+1) ×1 BPSC (BPSC-A, BPSC-B), three groups of wavelength stabilized laser diodes (LDs), respectively. The center wavelength of LDs is 976 nm, and the maximum output power of each group is about 900W. The core/cladding diameters of the output pigtail of the LDs are 220/242 μm. The core/cladding diameters of the pump output fiber and signal output fiber of BPSC (BPSC-A, BPSC-B) is 25/400 μm and 25/250 μm, respectively. The length of pumping fiber and signal output fiber of BPSC-A is about 2.6 m and 1.2 m, respectively. The length of pumping fiber and signal output fiber of BPSC-B is about 1.7 m and 1.0 m, respectively. Each three groups' LDs is coupled into DCYDFA and DCYDFB through BPSC-A and BPSC-B respectively. DCYDFA and DCYDFB are directly fusion spliced with OCFBG-A and OCFBG-B, respectively. The output laser of end A and end B separately transmit through a 3.3m-long passive fiber with a 15 cm-long CLS-A and a 2.9m-long passive fiber with a 15 cm-long CLS-B. The core/cladding diameters of passive fibers are both 25/400 μm. Subsequently, each end of output laser is injected into the measuring system which involves a power meter (PM), an optical spectrum analyzer (OSA), an oscilloscope, and a beam quality (M^2) measuring equipment. The power, spectrum, beam quality, and temporal characteristics of the output laser are measured simultaneously.

IV. Experimental Results

A. Research on the Stability Characteristics of B-OAIFL

The stability characteristics of B-OAIFL were experimentally studied. Taking the A-end pumping as an example, the results are

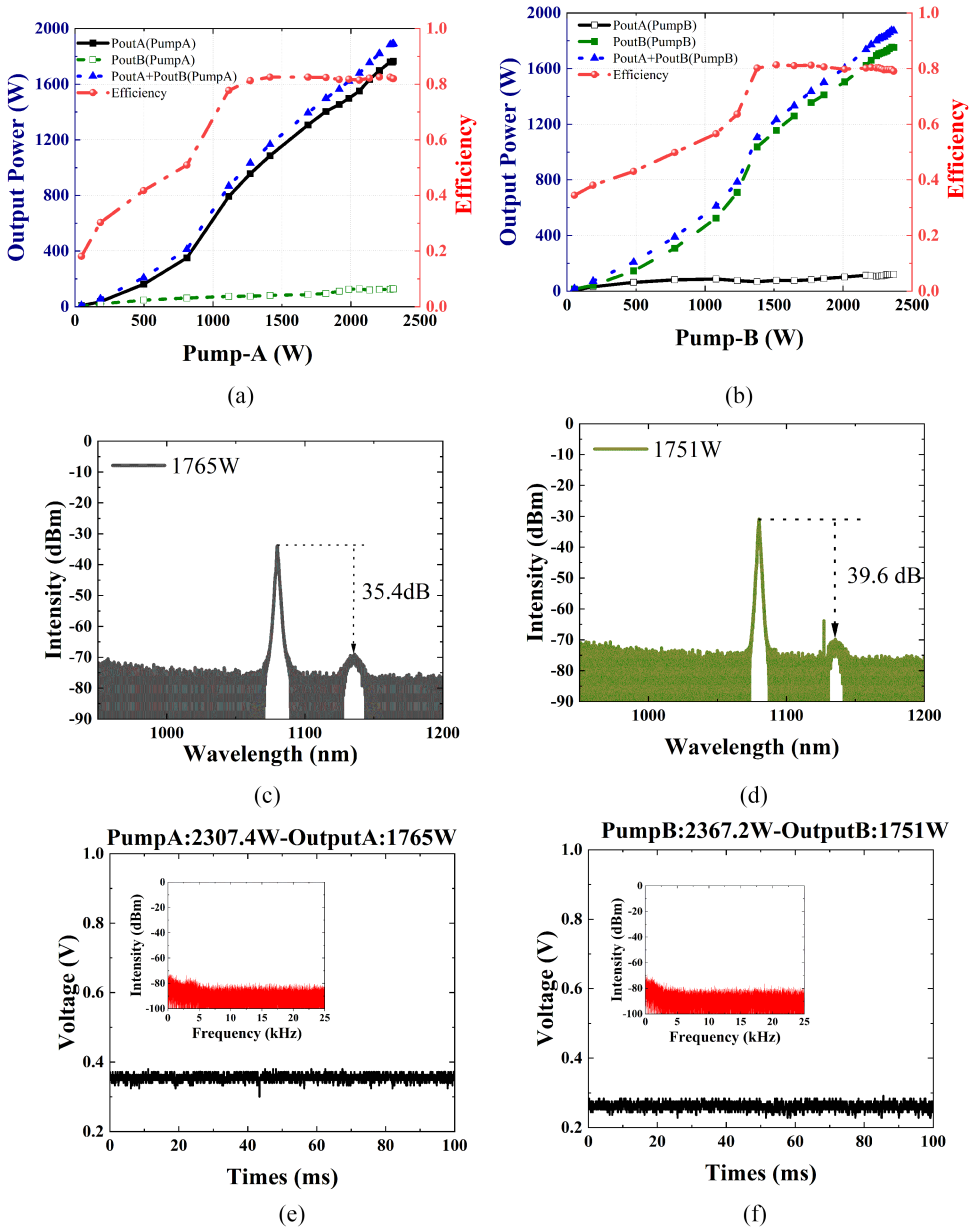

Fig. 8. Experimental results of unidirectional pumping: (a) The variation of A-end output power and efficiency with pump power under the A-end pumping; (b) The variation of B-end output power and efficiency with pump power under the B-end pumping; (c) The output spectrum of end A at its maximum output power; (d) The output spectrum of end B at its maximum output power; (e) The time-domain and its FFT results(inset) at the output power of end A of 1765 W; (f) The time-domain and its FFT results(inset) at the output power of end B of 1751 W.

shown in Fig. 7. The output signal of the photoelectric detector (PD) shows that there are pulses with high peak value in the output signal. At the same time, strong SRS appears in the spectrum, accompanied by high-order Stokes light. The result in spectrum and time domain indicates a significant instability of the B-OAIFL. The main reason is that the pump power is relatively low, and it is almost completely absorbed by the active fiber when it passes through the amplifying section, such a process leads to a low power level of the oscillating section, and results in a certain degree of ASE and self-excited oscillation of the amplifier which makes the instability of the laser. From the previous work, we know that the laser can be stabilized by increasing the power of oscillating section continually. So we further increase the pump power, and finally the laser stabilizes at a power of 1086 W. At this time, no SRS is observed on the output spectrum.

B. Experiment Results of Unidirectional Pumping

Firstly, we apply unidirectional pumping configuration to the laser and experimentally studied the characteristics of the output laser of B-OAIFL, the results are shown in Fig. 8. Fig. 8(a), (b) shows the variation of output power and efficiency with pump power under the condition of the unidirectional pumping.

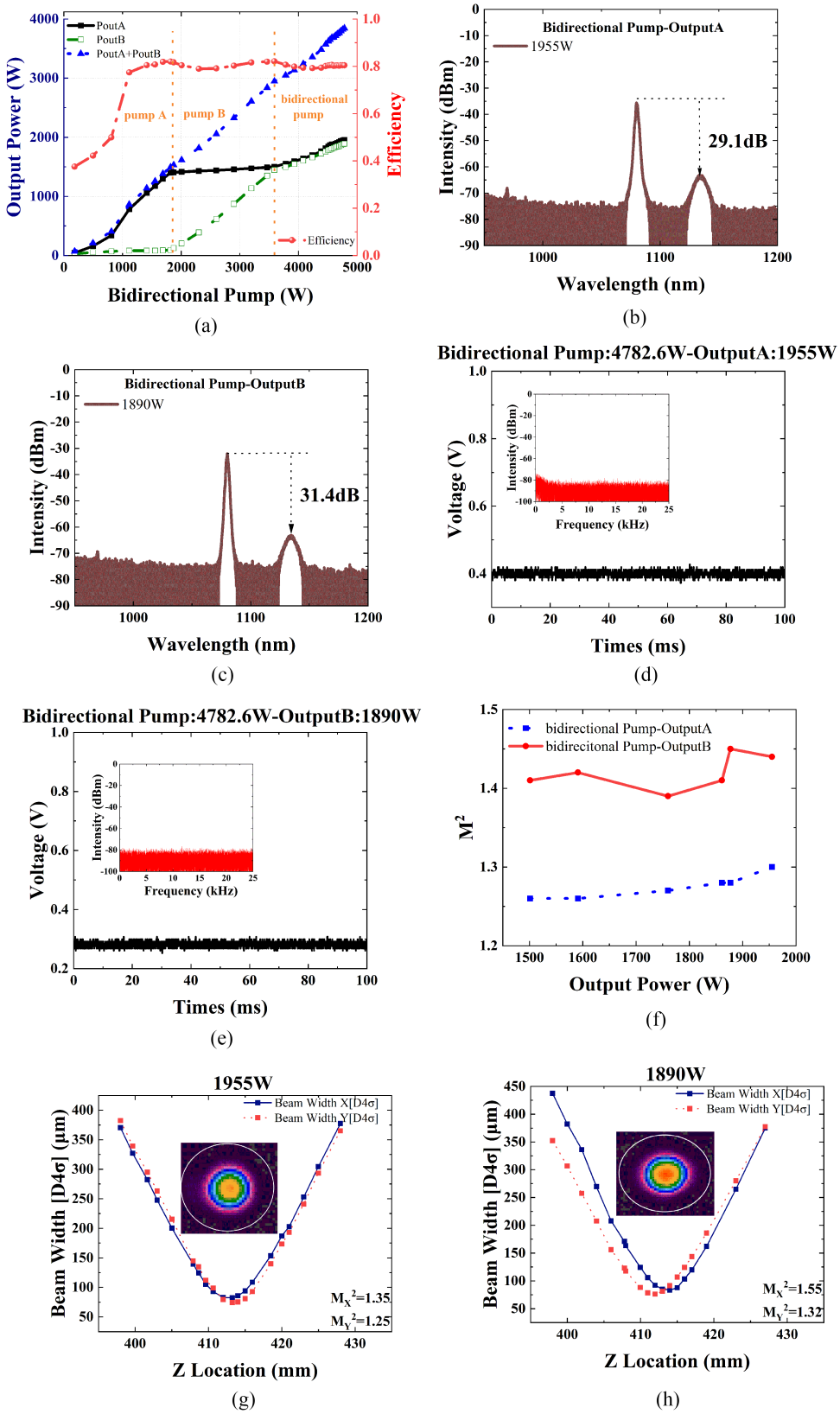

Fig. 9. Experimental results under bidirectional pumping: (a) The variation curve of output power and efficiency with bidirectional pump power; (b) The output spectrum at the maximum power of end A; (c) The output spectrum at the maximum power of end B; (d) The time-domain and its FFT results(inset) of end A at 1955 W; (e) The time-domain and its FFT results(inset) of end B at 1890 W; (f) The variation of M^2 with the output power; (g) The beam quality factor M^2 at the A-end output power of 1955 W (inset: the beam profile); (h) The beam quality factor M^2 at the B-end output power of 1890 W (inset: the beam profile).

When A-end pumping is applied, the output power of end A and total output power have an approximately linear increase with the increase of pump power, while the output power of end B keeps in a low level with a small increase. The main reason is that the pump light is almost fully absorbed by DCYDFA and DCYDFO, almost no pump light can enter DCYDFB to amplify the signal output from end B. In terms of the O-O efficiency, it initially increases with the increasing pump power and then gradually stabilizes and finally shows a small decrease. The same phenomenon occurs under the B-end pumping, as is shown in Fig. 8(b). Fig. 8(c), (d) show the output spectrums of end A and end B, respectively. Under the condition of A-end pumping, the maximum output power of end A of 1765 W and end B of 127 W is achieved. The total output power is 1892 W with an O-O efficiency of about 82.0% at a pump power of 2307.4 W. The intensity of SRS is 35.4 dB lower than the signal light with a 3 dB bandwidth of 0.9 nm. Besides, under the condition of B-end pumping, the maximum output power of end B is 1751 W with an O-O efficiency of about 79.04% when the total pump power is 2367.2 W. At this case, the SRS intensity is about 39.6 dB lower than that of the signal light. Fig. 8(e), (f) depict the time-domain characteristics of output laser of end A and end B at its maximum power, respectively. Obvious characteristics of TMI are observed in the temporal property of signal and its corresponding fast Fourier transform (FFT) results. The further scaling of laser output power under the condition of unidirectional pumping is limited by TMI.

C. Experiment Results of Bidirectional Pumping

Next, we demonstrate the structure under the condition of bidirectional pumping, the characteristics of the output laser are studied in detail. We initially adopted the method of bidirectional simultaneous pumping, a severe ASE, however, was observed, which mainly due to insufficient pump light reaching the oscillating section. For the sake of security, we changed the power source configuration. In the new pump configuration, we first turned on the pump source of end A to reach the stable state of the laser. Subsequently, the pump of end B is increased to an approximate power level to A-end pumping. Finally, we adopted the bidirectional simultaneous pumping, the results are shown in Fig. 9. A bidirectional total output power of 3845 W (1955 W of end A, 1890 W of end B) is achieved with an O-O efficiency of 80.4% while the total pump power is 4782.6 W (2415.4 W of end A, 2367.2 W of end B). Due to the difference of device parameters and pump power between end A end and end B, the output power of both ends of the laser is slightly different. As is depicted in Fig. 9(b), (c), the intensity of SRS of end A and end B are 29.1 dB and 31.4 dB lower than the signal light at their maximum output power with the 3-dB bandwidth of 1.78 nm and 1.56 nm, respectively. We can see from the Fig. 9(d), (e) that obvious TMI features are observed in the time domain and its FFT results at end A, without any TMI features at end B. Fig. 9(f) shows the results of the beam quality(M^2 factor) of the output laser of end A and end B at different output power. The beam quality of end A and end B at the highest output power is $M_X^2 = 1.35, M_Y^2 = 1.25$ and $M_X^2 = 1.55, M_Y^2 = 1.32$, respectively. The further scaling of laser output power under the condition of bidirectional pumping is limited by TMI.

An obvious SRS can be observed in no matter unidirectional pumping or bidirectional pumping scheme. According to the physical analysis of the SRS, we know that it may cause by overlong fiber or small core diameter. However, the total length of the active fiber in our experiment is about 20 m, considering the characteristics of the B-OAIFL, the pump light of one end has little influence on the other end, so the length of the active fiber can be regarded as 13 m, which can not sufficiently result in such obvious SRS according to our previous experience, so we believe that the emergence of the SRS in our experiment may be caused by the temporal instability that is thought to still exist in the cavity, therefore in future work we will focus on optimizing the parameters to achieve a more stable cavity state, and eliminate its potential impact on the emergence of SRS.

IV. Conclusion

A B-OAIFL was proposed for the first time, and the feasibility of this structure was successfully verified experimentally. By using the SeeFiberLaser simulation software, we obtained the function of the output power and efficiency with the reflectivity and center wavelength of FBGs, which theoretically guides the selection of the FBGs. With an active fiber length of 6 m for the oscillating section and 7 m for the amplifying section at both ends, a bidirectional 2-kW-level output oscillating-amplifying integrated fiber laser was demonstrated with an O-O efficiency of 80.4%. The advantages of the bidirectional output fiber laser oscillator and the oscillating-amplifying integrated fiber laser are inherited. Besides, based on the analysis of the structure, the B-OAIFL should theoretically have a higher efficiency due to the better utilization of the pump light. Moreover, it is believed to have a lower requirement of FBGs and an ability of simple adjustment for output power of each end. The further scaling of the output power is limited by the TMI. In future work, we will devote to optimizing the structural design of the bidirectional output oscillating-amplifying integrated fiber laser to obtain a further improvement in TMI threshold and efficiency. In addition, the length distribution of the oscillating section and the amplifying section will be further optimized to obtain a lower stability threshold of laser.

Acknowledgment

Thanks Xiaoyong Xu, Siliu Liu, Yun Ye, Li Wang, Yujun Wen, Penglin Zhong, Xiangming Meng, Fengchang Li in the help of the experiment.

References

[1] D. J. Richardson, J. Nilsson, and W. A. Clarkson, "High power fiber lasers: Current status and future perspectives [Invited]," *J. Opt. Soc. Amer. B*, vol. 27, pp. B63–B92, 2010.

[2] J. Nilsson and D. N. Payne, "High-power fiber lasers," *Science*, vol. 332, no. 6032, pp. 921–922, 2011.

[3] M. N. Zervas and C. A. Codemard, "High power fiber lasers: A review," *IEEE J. Sel. Topics Quantum Electron.*, vol. 20, no. 5, pp. 219–241, Sep./Oct. 2014.

[4] M. N. Zervas, "High power ytterbium-doped fiber lasers — Fundamentals and applications," *Int. J. Modern Phys. B*, vol. 28, no. 12, 2014, Art. no. 1442009.
[5] Z. Lin, Y. Wang, J. Xu, and J. Wu, "Analysis of influence of fiber coupler on the performance of optical system," *Electro-Optic Technol. Appl.*, vol. 36, 2021, Art. no. 26.
[6] L. Dai, "Carbon dioxide gas laser with bidirectional laser out-put," CN2398750Y, Sep. 2000.
[7] S. Wan, Q. Tian, and L. Sun, "Experimental research on the stability and the multi-longitudinal mode interference of bidirectional outputs of LD-pumped solid-state ring laser," *Materials, Act. Devices, Opt. Amplifiers*, pt. 2, 2003.
[8] C. H. Liu et al., "810W continuous-wave and single transverse-mode fibre laser using 20 μm core Yb-doped double-clad fibre," *Electron. Lett.*, vol. 40, pp. 1471–1472, 2004.
[9] J. Jiang et al., "Bidirectional ultrahigh-repetition-rate ultrafast fiber laser," *Opt. Laser Technol.*, vol. 142, 2021, Art. no. 107196.
[10] W. Cui, X. Zhou, M. Bi, G. Yang, M. Hu, and T. Wang, "Switchable generation of multi-wavelength continuous wave and square-wave pluses in a bidirectional Erbium-doped fiber laser," *Opt. Laser Technol.*, vol. 143, 2021, Art. no. 107302.
[11] G. Hu, M. Dong, K. Chen, Z. Wang, H. Niu, and L. Zhu, "Tunable multidimensional multiplexed Q-switched pulse outputs from a linear fiber laser with a bidirectional loop," *Opt. Laser Technol.*, vol. 141, 2021, Art. no. 107138.
[12] D. Xue and L. Xu, "A single-fiber linear cavity double-end output all-fiber laser," CN107508124A, Dec. 2017.
[13] X. Wang et al., "A linear cavity all-fiber laser oscillator with adjustable bidirectional output power," CN208820223U, May 2019.
[14] P. Zhong et al., "2 $\times$ 2 kW near-single-mode bidirectional high-power output from a single-cavity monolithic fiber laser," *Opt. Lett.*, vol. 47, no. 11, pp. 2806–2809, 2022.
[15] K. Hejaz et al., "Transverse mode instability threshold enhancement in Yb-doped fiber lasers by cavity modification," *Appl. Opt.*, vol. 57, pp. 5992–5997, 2018.
[16] L. Zeng, X. Wang, B. Yang, H. Zhang, and X. Xu, "A 3.5-kW near-single-mode oscillating–amplifying integrated fiber laser," *High Power Laser Sci. Eng.*, vol. 9, no. 3, pp. 58–64, 2021.
[17] Q. Shu et al., "2 kW class antireflection fiber laser with oscillator-amplifier integration," *Chin. J. Lasers*, vol. 45, 2018, Art. no. 0801004.